Simulations of the Solution Structure of HIV-1 Protease in the Presence and Absence of Bound Zinc

D. M. YORK,[1,2]* L. J. BARTOLOTTI,[3] T. A. DARDEN,[1] L. G. PEDERSEN,[1,2] and M. W. ANDERSON[1]

[1]*Laboratory of Molecular Toxicology, National Institute of Environmental Health Sciences, Research Triangle Park, North Carolina 27709,* [2]*Department of Chemistry, University of North Carolina, Chapel Hill, North Carolina, 27599-3290, and* [3]*North Carolina Supercomputing Center, a Division of MCNC, Research Triangle Park, North Carolina 27709*

Received 8 June 1993; accepted 3 August 1993

ABSTRACT

Zinc ions have been shown to inhibit human immunodeficiency virus type 1 (HIV-1) protease *in vitro* at neutral pH [Zhang et al. *Biochemistry,* **36,** 8717 (1991)]. Kinetic data from this study support a reversible binding mechanism of zinc in the active site. Preliminary calculations of the ion–protein potential energy based on the geometry of the crystallographic structure [Wlodawer et al. *Science,* **245,** 616 (1989)] are consistent with this proposed mechanism. To examine the structure of HIV-1 protease with zinc bound in the active site, molecular dynamics simulations in the presence and absence of zinc at this site have been carried out to 200 ps. These simulations suggest zinc remains stably bound to the catalytic aspartate residues without disruption of the dimer or significant alteration of the active site structure. These data are consistent with those observed by Zhang et al. (1991), and together give strong evidence that this is the binding site that leads to inactivation. A proposed model of zinc binding at the active site based on quantum mechanical calculations indicates Zn^{+2} coordination is monodentate with each catalytic aspartate, leaving at least two ligand positions potentially free (occupied by water molecules in the calculations).

Introduction

Human immunodeficiency virus type 1 protease (HIV-1 PR) is a virally encoded enzyme essential in the maturation process of the HIV-1 retrovirus. HIV-1 PR is a dimeric aspartyl protease[1] that mediates the proteolytic cleavage of the viral *gag* and *gag-pol* fusion polyproteins into their functional forms.[2] Consequently, HIV-1 PR is required for viral infectivity, making it an attractive thera-

*Author to whom all correspondence should be addressed.

CCC 0192-8651/94/001061-11

peutic target.[3,4] The elucidation of X-ray crystal structures of the enzyme both unbound[5–7] and bound to synthetic inhibitors[8] has greatly enhanced the current understanding of the structure and inhibitory mechanism of HIV-1 PR.

A striking difference between the HIV-1 protease and cellular proteases is seen in the pH dependence of its activity. The optimum pH range for activity of the HIV-1 protease (4.5–6.0)[9] is higher than for cellular enzymes *in vitro* (typically 2.0–4.0).[10] An exception is human renin,[11] which has optimum activity between pH 5.5–7.5. The pH dependence of these enzymes presumably reflects the catalytic mechanism generally accepted for aspartyl proteases, which requires one of the two catalytic aspartate residues to be protonated. The unusually high pH optima of HIV-1 PR and renin is due, at least in part, to substitution of an alanine residue in the position immediately following the active site triad (residues 25–27, HIV-1 PR numbering). In most cellular aspartyl proteases, this residue contains a hydroxyl group (Ser or Thr) that can form a hydrogen bond with the carboxylate side chain of the catalytic aspartate and thereby stabilize the unprotonated form at lower pH.[10]

Recently, Zhang et al.[12] reported that zinc ions are inhibitors of both renin and HIV-1 PR at neutral pH. Although the zinc binding site(s) that leads to inactivation has not been conclusively determined, evidence suggests that one site may be at or near the catalytic aspartate residues in the active site. In this study, molecular dynamics (MD) has been used to explore the possibility of zinc binding in the active site of HIV-1 PR and predict the effects of this binding on the structure.

Methods

MD CALCULATIONS

Molecular mechanics and dynamics calculations were performed using a modified version of the AMBER3.0 (rev. A) software package[13] (rev. A by George Seibel, UCSF; for a description of code modifications, see ref. 14). The all-atom force field[15] was employed for all standard residues. Solvent was treated explicitly using the TIP3P water model.[16] Chloride ion parameters were obtained from Lybrand et al.[17] and zinc ion parameters were obtained from Bartolotti et al.[18] Electrostatic and van der Waals interactions were treated using a "twin range" (9/18-Å) residue-based cutoff, updated every 20 steps. Simulations were performed under constant temperature (300 K) and pressure (1 bar) conditions using a 1-fs integration time step and carried out to 200 ps. All calculations were performed on a Cray Y-MP supercomputer (National Cancer Institute or North Carolina Supercomputing Center) or in parallel on a Silicon Graphics Iris 4D/380-VGX workstation.

The starting positions of the heavy atoms for the unbound and Zn^{+2}-bound dimers were obtained from the crystallographic structure of the synthetic [$Aba^{67,95}$] HIV-1 protease,[6] crystallized at pH 7. The hydrogen positions were added with AMBER and relaxed with steepest descents energy minimization with the heavy-atom positions fixed. The net charge of the unbound dimer was assumed to be +4, consistent with the normal protonation state of the component amino acids at neutral pH. The catalytic state of the enzyme, however, requires one of the active site aspartate residues to be protonated while the other is unprotonated.[4] It is possible that the active site aspartates share a proton near neutral pH because maximum protease activity occurs in the range 4.5–6.0.[9] However, inflections in the log $[V_{max}/K_m]$ vs. pH profile observed at pH 3.1 and 5.2 suggest one of the aspartates deprotonates at pH 5.2.[9] Because we are interested in simulating the protease at neutral pH, we have chosen to treat both aspartates as being fully charged in the simulations. This treatment of the aspartates preserves the crystallographic C_2 symmetry of the dimer and is consistent with previously reported simulations of HIV-1 PR in the unbound form.[19,20] Further, for the case of the Zn^{+2}-bound protease it is reasonable to assume that Zn^{+2} ion binding would involve both aspartates in the unprotonated form.

Initial placement of a Zn^{+2} ion was determined by a grid search procedure, whereby the AMBER nonbond interaction energy (no cutoff) of the ion was tested on a 0.5-Å grid in a box at least 5.0 Å larger than the crystallographic structure. The grid points corresponding to the 1000 lowest energies were used as starting points for minimization of a single Zn^{+2} ion to an rms gradient tolerance of 1×10^{-6} kcal/mol. The position corresponding to the global potential energy minimum was chosen for the placement of the ion. This procedure resulted in optimal placement of the Zn^{+2} ion occuring in the active site cleft directly between the carboxylate side chains of the catalytic aspartate residues, in agreement with the binding site proposed by Zhang et al.[12] Other favorable minima

occurred near negatively charged aspartate and glutamate residues on the surface of the protease; however, these locations were significantly higher in energy than at the catalytic aspartates.

As computational techniques are able to treat long-range electrostatics more rigorously and thus provide for longer stable simulation, the condition of charge neutrality becomes increasingly important. To ensure that artifacts were not introduced into the simulation due to the charge state of the system, the net charge of the protease and protease:ion complex were neutralized with negatively charged chloride ions. Chloride ions were placed one at a time with the same procedure used for the Zn^{+2} ion. Hence, four chloride ions were added to the system containing the unbound protease and six chloride ions to the system containing the zinc-bound protease. Solvation was accomplished by immersing the protein/protein–ion coordinates in a large water box such that a layer at least 13 Å thick surrounded the solute. Water molecules were placed so as to have no water oxygen closer than 2.8 Å or water hydrogen closer than 2.0 Å to a protein atom or ion. This procedure resulted in 8013 water molecules for each system. The water molecules were relaxed with 200 steps of steepest descents minimization with the protein and ion positions fixed, equilibrated with 20 ps of MD, and reminimized with 200 steps of steepest descents minimization. Positional constraints on the solute and ions were then removed, and the entire system was relaxed with 200 steps of steepest descents minimization to give the starting configuration for molecular dynamics. Initial velocities were obtained from a Maxwellian distribution at 1 K, and stepwise heating to 300 K was performed over 10 ps. Unconstrained dynamics was then performed on each system at constant pressure and temperature to 200 ps.

QUANTUM MECHANICAL CALCULATIONS

Semiempirical quantum mechanical calculations were performed with MOPAC6.0[21] (Quantum Chemistry Program Exchange 455) using the PM3 Hamiltonian[22] (for a recent discussion of the quality of these parameters, see ref. 23). Heavy atoms of residues 24–27 of the crystallographic structure and the identical symmetry-related residues were used to model the active site. End groups and hydrogen atoms were then added to produce the unrefined active site model [CH_3-CO-Leu^{24}-Asp^{25}-Thr^{26}-Gly^{27}-NH-CH_3]$_2$. Initial positions for the zinc ion and nearby water molecules were obtained from the equilibrated zinc-bound protease (above). Geometry optimizations of the active site with a zinc ion and two, three, and four water molecules were performed, as well as with a hydronium ion (replacing the zinc ion) and two water molecules. Geometry optimizations were performed with the amino acid backbone atoms (-N-C_α-C-) anchored to their crystallographic positions. The convergence tolerance for the self-consistent field energy at each step of the geometry optimization was 1.0×10^{-10} kcal/mol. Optimizations were terminated when the relative change in the gradient norm between steps became less than 0.01.

Results

A comparison of the overall structure and fluctuations of the HIV-1 PR dimer in solution in the absence of zinc (MDS) and with zinc bound to the catalytic aspartates (MDZn) have been made based on molecular dynamics simulations. A refined model of the active site based on quantum mechanical calculations is also presented. These results support the original suggestion of Zhang et al.[12] that this is the probable binding site of zinc that leads to inhibition of HIV-1 PR and give detailed structural insight into the nature of this binding.

GENERAL STRUCTURAL FEATURES

The time evolution of the rms deviation of α carbon atoms with respect to the crystallographic structure for MD structures of the unbound (bold line) and Zn^{+2} bound (thin line) protease are shown in Figure 1. Both systems are well equilibrated after 150 ps. The unbound protease equilibrates with an α carbon rms deviation of ~1.5 Å, whereas the Zn^{+2}-bound structure equilibrates at a slightly lower value of ~1.2 Å. Analysis of atomic fluctuations (α carbons) is shown in Figure 2. Corresponding fluctuations in the crystallographic structure can be estimated from the isotopic temperature factors (B values) through the relation[24]

$$\langle \Delta \mathbf{r}_i^2 \rangle^{1/2} \equiv [\langle \mathbf{r}_i^2 \rangle - \langle \mathbf{r}_i \rangle^2]^{1/2} = \left[\frac{3}{8\pi^2} B_i\right]^{1/2} \quad (1)$$

where $\mathbf{r}_i$ is the position vector of atom i in the simulations and B_i is the corresponding crystallographic temperature factor. Fluctuations derived from the crystallographic temperature factors

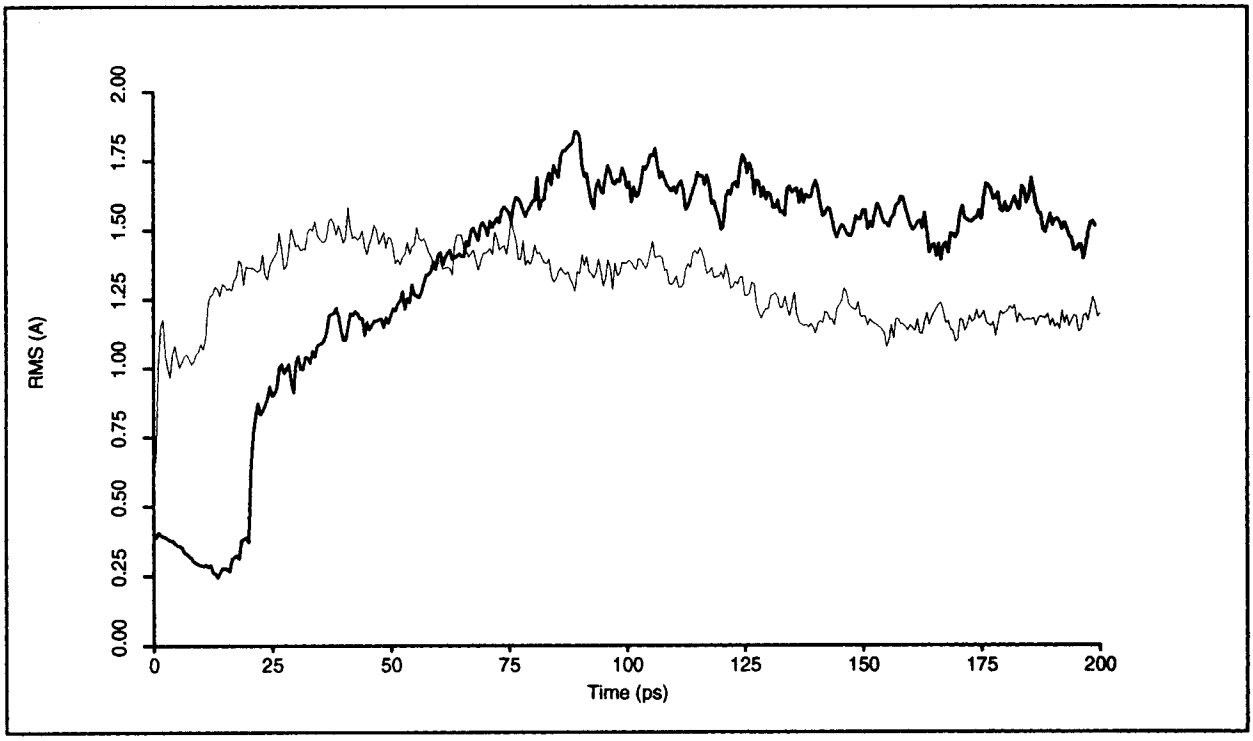

FIGURE 1. Time evolution of the α carbon rms deviation from the crystallographic structure[6] for MDS (bold line) and MDZn (thin line).

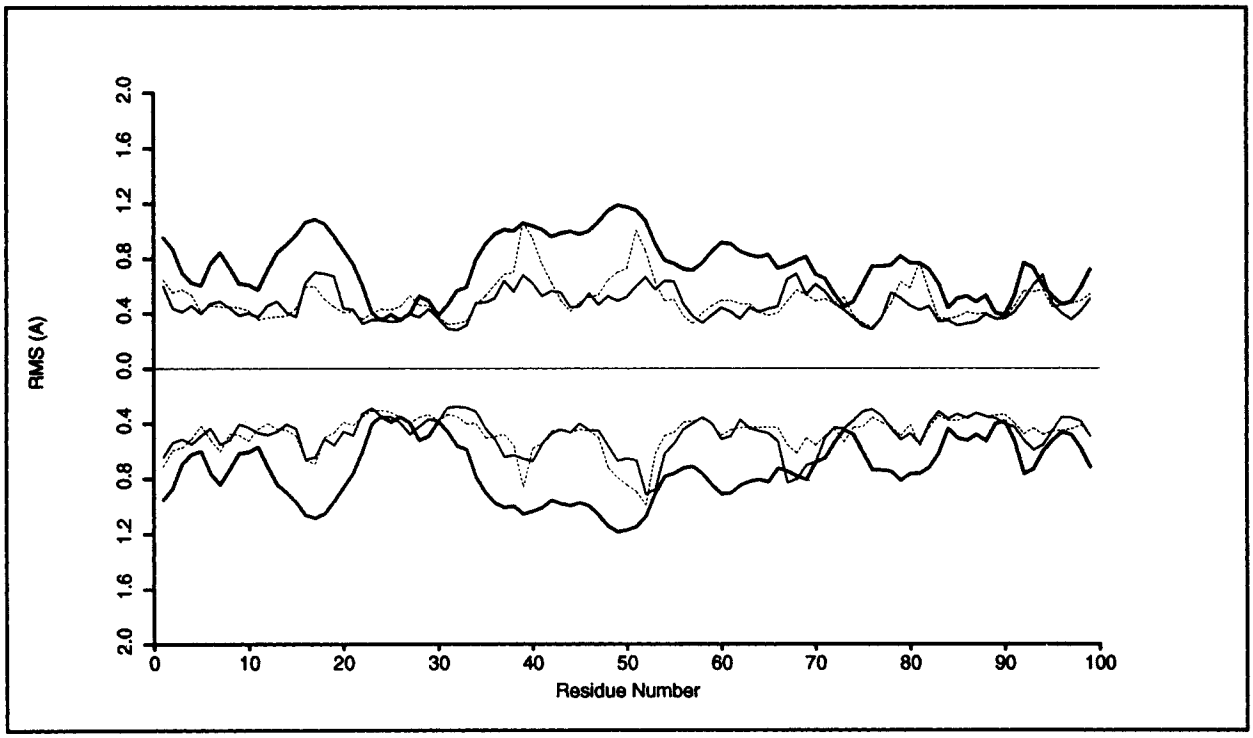

FIGURE 2. Comparisons of the rms fluctuations [eq. (1)] calculated from the simulations (MDS, thin solid line; MDZn, broken line) and estimated from the crystallographic temperature factors (bold line). Monomer 1 is shown above the abscissa and monomer 2 below.

(thick solid lines, Fig. 2) and fluctuations computed over the last 50 ps of the simulations for MDS (thin solid lines) and MDZn (broken lines) are shown. Fluctuations computed from the simulations are qualitatively similar to those derived from the crystallographic temperature factors, with the notable difference that the former are generally smaller in amplitude. This phenomena has also been observed in other simulations of HIV-1 PR.[25] To account for this discrepancy, it has been suggested that the fluctuations derived from the crystallographic data are artificially large because symmetry constraints used in the refinement lead to an overestimate of the thermal factors. It is possible, however, that the simulation period is not sufficiently long to adequately sample all the important local conformational minima, and hence the calculated fluctuations represent a somewhat restricted region of conformational space.

Analysis of the secondary structure was performed using the Kabsch and Sander program DSSP.[26] The secondary structural assignments are remarkably similar. Of the 63 secondary structural assignments made for the crystallographic monomer, 46 (73%) were conserved in each monomer of the 150 to 200-ps average structure of the unbound protease (<MDS>) and 54 (86%) were conserved in each monomer of the Zn^{+2}-bound average structure (<MDZn>). Among these included regions at the amino and carboxyl termini (residues 2 and 3, 96–98), the loop formed by the *b* and *c* β chains (residues 10–24), residues 43–46 and 55–59 at the base of the flaps, and the region of the *h'* helix (residues 87–94) (for reference to the secondary structural domains, see refs. 6 or 20).

The early refolding of the protease backbone in each of the solution simulations can be examined by superimposing the simulation average structures onto the crystallographic structure. The overall rms deviation for 198 α carbon atoms was 1.46 Å for <MDS> and 1.06 Å for <MDZn>. The largest deviation occurs in the flap region of the protein (residues 42–58). Comparison of the protease structure in a crystalline environment and in solution shows that the flaps refold upon solvation due to the loss of a crystal packing contact between the flaps of one dimer and the *h'* helix of a neighboring dimer.[20] Other regions of large deviation (residues 7, 67 and 68, and 80–82) occur in loops and turns that connect regions of secondary structure (β chains), and generally correlate with regions of high fluctuation (see Fig. 2).

HYDROGEN BONDING

Analysis of the hydrogen bond structure of protease in the presence and absence of zinc has been performed over the final 50 ps of the simulations. A detailed presentation of hydrogen bonding and solvation structure in the unbound simulation has been previously reported.[20] An expanded version of the article that contains a complete analysis of hydrogen bonding observed in the simulations is available upon request.

The primary hydrogen bond interactions at the dimer interface present in the crystallographic structure are maintained in the simulations (Table I). These include interactions at the amino and carboxyl terminal β strands (residues 1–4, 95–99), which form a four-stranded antiparallel β sheet, and in the region of the active site triads (residues 25–27), which interlock in the so-called "fireman's grip" characteristic of aspartyl proteases.[27] In addition, intersubunit hydrogen bonding between the tips of the flaps was observed in the unbound simulation. Similar H bonding has previously been predicted from analysis of crystallographic data.[6]

ZINC–PROTEIN INTERACTIONS

The pair distribution function for the carboxylate oxygens of the catalytic asparate residues around the Zn^{+2} ion (not shown) has a single sharp peak centered around 2.13 Å. The corresponding coordination number of carboxylate oxygens is 4. The pair distribution function for water oxygens around the Zn^{+2} ion (not shown) has two ordered solvation shells. The first is a fairly sharp peak centered around 2.25 Å, with coordination number 3. The second solvation shell is more broad and centered at approximately 4.4 Å. No exchange of oxygens (water or carboxylate) was observed in the first coordination shell during the last 50 ps of the simulation. This is not unexpected because the lifetime of a water molecule in the coordination sphere of a zinc ion is estimated to be on the order of a nanosecond.[28]

To probe the structure of zinc ion binding in the active site of HIV-1 PR in greater detail, quantum mechanical calculations were performed using MOPAC6.0 (see the methods section). The active site triads were modeled by the modified peptide sequences $[CH_3\text{-}CO\text{-}Leu^{24}\text{-}Asp^{25}\text{-}Thr^{26}\text{-}Gly^{27}\text{-}NH\text{-}CH_3]_2$. Calculations were directed at modeling the interactions of the zinc ion with the carboxylate side chains of the catalytic aspartate residues be-

TABLE I.
Hydrogen Bonding at the Dimer Interface.

		Zn^{+2} Bound		Unbound	
Contact Atom 1—Atom 2	X-Ray Dist. (Å)	⟨Dist⟩ (Å)	% Time Bonded	⟨Dist⟩ (Å)	% Time Bonded
Pro^{1} HN^{+}—Phe^{99} O	1.71	1.79	100	1.73	100
		1.76	100	2.85	46
Pro^{1} O—Phe^{99} HN	2.16	2.13	86	2.07	93
		—	—	—	—
Ile^{3} HN—Leu^{97} O	1.68	2.12	88	2.09	88
		2.12	88	2.03	93
Ile^{3} O—Leu^{97} HN	1.78	1.97	97	1.97	99
		1.96	100	1.97	99
Leu^{5} O—Arg^{87} HN21	2.16	1.97	96	2.03	87
		1.91	98	3.39	28
Trp^{6} O—Arg^{87} HN22	—	2.23	66	2.60	16
		2.09	88	3.81	13
Leu^{24} O—Thr^{26} HOG	2.55	1.90	99	2.05	93
		1.88	100	1.91	100
Thr^{26} HN—Thr^{26} OG1	2.22	2.02	98	2.29	65
		2.05	98	2.03	93
Gly^{49} HN—Gly^{51} O	—	—	—	2.06	94
		—	—	—	—
Gly^{51} HN—Gly^{51} O	2.42	—	—	1.99	100
		—	—	—	—
His^{69} HNE—Phe^{99} OXT^{-}	2.49	—	—	—	—
		1.99	89	—	—
Thr^{96} HN—Asn^{98} O	2.41	2.03	93	2.00	98
		2.03	95	2.01	99
Thr^{96} O—Asn^{98} HN	2.02	2.00	98	1.94	99
		2.03	93	1.96	99

Hydrogens were added to the crystallographic structure (X-ray) using AMBER and energy minimized keeping the nonhydrogen positions fixed. In the unbound and Zn^{+2}-bound simulations, the average H-bond distances (⟨Dist⟩), and percentage time the H bond was maintained [% Time Bonded; definition of an H bond is the same as in ref. 20] are listed for each monomer (monomer 1 is listed on the same line as the H-bond atoms; monomer 2 is listed immediately below).

cause these were the only ion–protein interactions observed in the MD. Backbone atoms were constrained to their crystallographic positions in all optimizations to preserve the overall protein structure. Because the active site is located at the dimer interface in the core of the protein, it is reasonable to expect restricted backbone mobility in this region. Inspection of the isotropic temperature factors (B values) shows that the average B value for the backbone (-N-C_α-C-) atoms of the active site (residues 24–27; $\langle B \rangle$ = 3.49 Å^2) is significantly lower than for the overall backbone average (15.72 Å^2). This corresponds to an rms fluctuation of 0.36 Å, suggesting backbone atoms in this region fluctuate in a relatively restrictive potential of mean force.

Before considering zinc binding in the active site, we first tested the peptide model in the absence of zinc for comparison with the crystallographic structure. In the active enzymatic form, it is generally believed that a proton is shared between the two catalytic aspartate residues and a nearby water molecule.[10] At neutral pH, the protonation state of the catalytic aspartate residues is not clear, and hence assignment of a particular bond structure involving the hydrogen may be somewhat ambiguous. Nonetheless, we have observed that a representation of the active site with both catalytic aspartates unprotonated and coordinating a single hydronium ion agrees closely with the crystallographic structure (Fig. 3a). It is possible that the actual structure near neutral pH involves a rapid equilibrium between several different protonation states.

Structures of the active site in the presence of zinc and two, three, and four water molecules in-

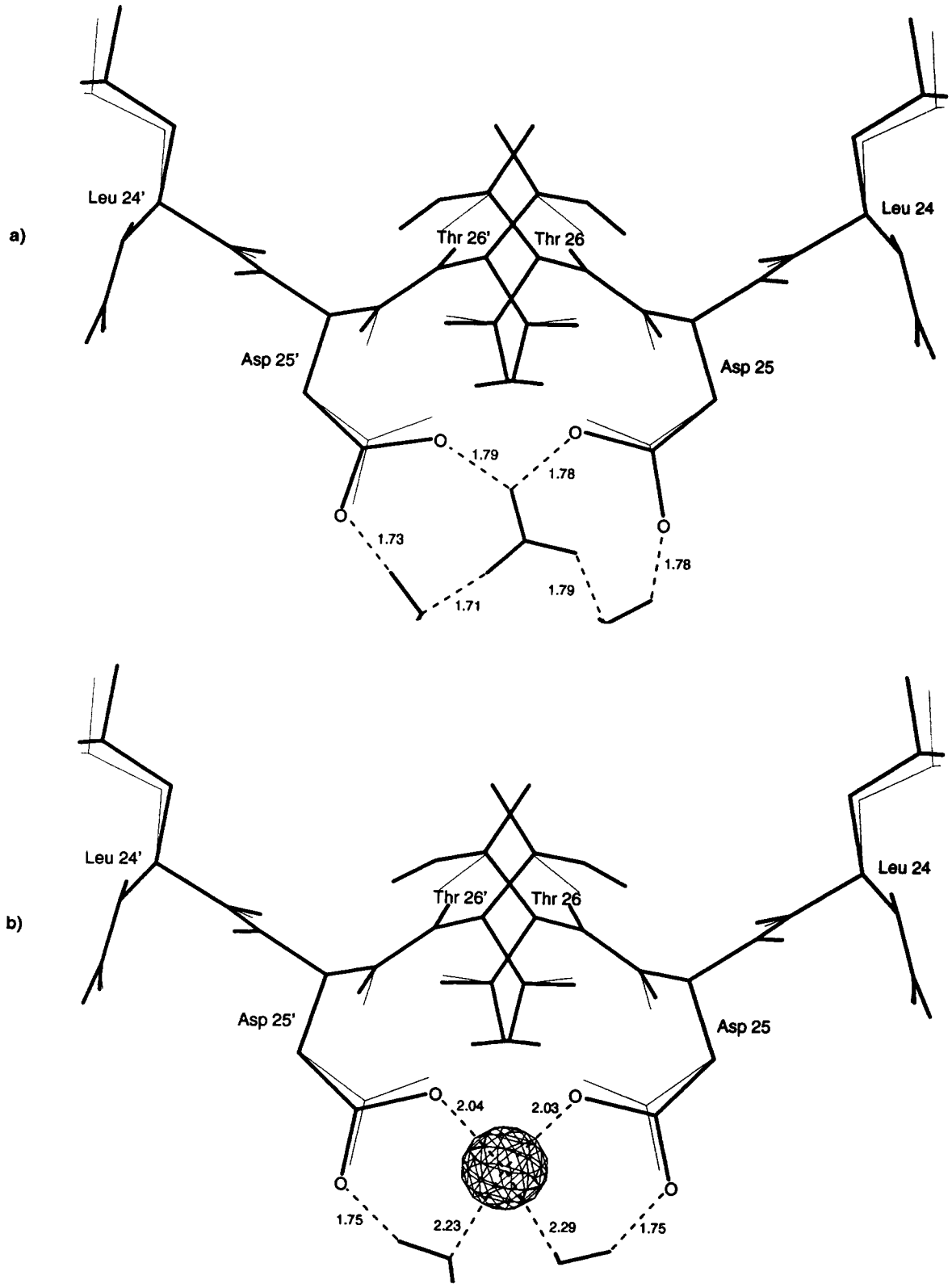

FIGURE 3. Energy-optimized structure (PM3 Hamiltonian) of the HIV-1 PR active site (thick lines) with (a) a hydronium ion and two water molecules and (b) a zinc ion and two water molecules. The plane of the illustration roughly coincides with the plane of the carboxylate groups of the catalytic aspartates. The corresponding atoms of the crystallographic structure are shown superimposed (thin lines). Hydrogen bond and ionic interactions are indicated by broken lines.

itially associated with the zinc ion were obtained from geometry optimizations using initial positions from the equilibrated MD results with the protein atoms constrained to their crystallographic positions. The structure of the active site in the presence of the zinc ion and two waters (Figs. 3b and 4) was similar to that of the hydronium ion structure. Two of the carboxylate oxygens, one from each aspartate residue, occupied ligand positions with the zinc. Two additional ligand positions were occupied by water molecules. Inclusion of three and four water molecules did not change the zinc coordination (i.e., no additional water molecules or carboxylate oxygens were observed within 2.5 Å of the zinc following optimization), and the structures were highly similar (data not shown). In the crystallographic structure, the carboxylate groups are nearly planar (angle "ϕ" between vectors normal to the planes of the carboxylates was 6°), with the OD1 oxygens of opposite residues in close proximity (O—O distance 3.1 Å). These features were slightly perturbed in the hydronium ion structure ϕ = 25°; O—O distance 2.9 Å), but were maintained in the zinc-bound structure ϕ = 2°; O—O distance 3.1 Å). The orientation of the carboxylates is stabilized by strong hydrogen bond interactions between the NH group of $Gly^{27}/Gly^{27'}$ and the OD1 atoms of the aspartate side chains in the optimized structures and in the crystallographic structure.

Our model of zinc binding to the carboxylate groups of the catalytic aspartate residues is consistent with studies of zinc ion binding to carboxylates based on small molecules in the Cambridge Structural Database. Carrell et al.[29] reported that zinc ions are generally observed bound in the plane of the carboxylate (the plane defined by the O-C-O atoms), in the *syn* orientation (70.1% of 67 compounds). In the proposed model, the zinc ion is nearly planar with the carboxylates (0.45 and 0.25 Å out of plane), and coordination is *syn* (57.6°, 55.3°). The mean Zn^{+2}—O distance observed by Carrell et al.[29] for 67 cases was 2.05 Å, near our calculated distances of 2.03 and 2.04 Å.

The observation that the model predicts formation of two stable contacts between the zinc ion and the catalytic aspartate side chains, leaving two ligand positions potentially free (occupied by water molecules in the model), suggests a possible pharmaceutical strategy. Design of zinc compounds with ligands that accommodate the steric and electrostatic requirements of the S3-S3′ subsites,[30] and that have favorable membrane transport properties,[31] may lead to new potent, selective inhibitors.

Discussion

The results presented here are consistent with experimental data[12] and suggest that inhibition of the HIV-1 protease by Zn^{+2} ions occurs via binding to the catalytic aspartate residues of the active site. Kinetic studies have shown that zinc is an effective inhibitor of renin and the HIV-1 protease at pH 7, two aspartyl proteases with pH optima near neutrality.[12] Other studies of metal ion inhibition of HIV-1 protease performed at pH 5 did not reveal significant inhibition of the enzyme by Zn^{+2} ions.[32] If inhibition of HIV-1 PR is a result of Zn^{+2} binding at the active site aspartate residues, it is reasonable to expect that conditions that favor both aspartates in the unprotonated form would enhance Zn^{+2} binding and hence inhibition. Because both catalytic aspartates are presumably unprotonated around neutrality, the observed pH dependence of Zn^{+2} inhibition is consistent with binding at or near the catalytic aspartates. Although the bacterially expressed HIV-1 PR has three residues that commonly bind zinc (Cys^{67} His^{69} and Cys^{95}), Zn^{+2} also inhibits the related HIV-2 protease, which does not contain cysteines or histidines, in an identical manner as the HIV-1 protease,[12] suggesting these residues are not required binding sites for inactivation by zinc. Taken together with the fact that inhibition was observed to be first order in $[Zn^{+2}]$, it may be inferred that there is a single important binding site that causes inactivation.[12] Further, Zn^{+2} binding responsible for inactivation of the protease was observed to occur reversibly because protease activity could be restored upon addition of EDTA, which has a higher affinity than carboxylate moieties for Zn^{+2} ions. These data are, therefore, consistent with the requirement of noncovalent binding of zinc in the active site.

In proteins, zinc ions are predominantly observed to be associated with cysteine and histidine residues, and frequently with one aspartate or glutamate residue. However, protein structures exist, such as the DNA polymerase I from *Escherichia coli*, where zinc is found to be coordinated to three carboxylate moieties.[33] It has been observed that metal ion binding to proteins generally occurs in hydrophilic regions that are immediately surrounded by hydrophobic groups.[34] The catalytic aspartate res-

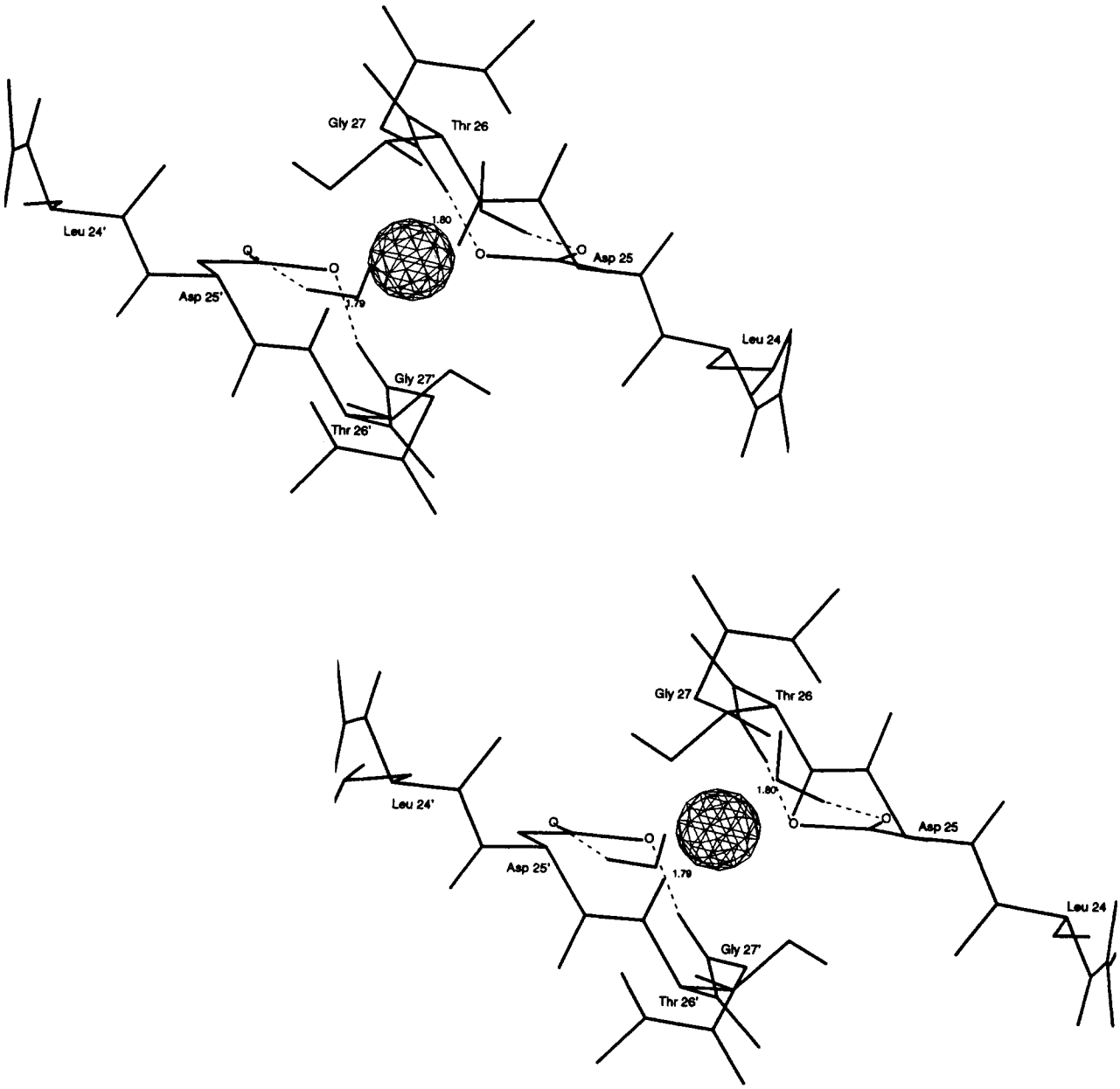

FIGURE 4. Stereo picture of the optimized structure (PM3 Hamiltonian) of the zinc-bound active site. Hydrogen bonds are indicated by broken lines. Small circles indicate positions of the carboxylate oxygens.

idues, located in the hydrophobic core of the HIV-1 protease, are consistent with this pattern.

The present study of Zn^{+2} binding at the catalytic aspartate residues provides a consistent view that this is the site responsible for inactivation of HIV-1 PR. Initial energetic considerations of the crystallographic structure are consistent with a favorable binding region for a Zn^{+2} ion in the active site at the catalytic aspartates (see the methods section). Molecular dynamics simulations predict the Zn^{+2} ion can remain stably bound at this site, i.e., no exchange of carboxylate oxygens was observed in the first coordination sphere of the zinc ion after equilibration. Because the hydrolysis mechanism mediated by HIV-1 PR presumably requires one of the aspartates to be protonated and the other to be unprotonated to activate a water molecule for hydrolysis,[4] the coordination of both of these residues

by a zinc ion would conceivably inactivate the enzyme. Inhibition of HIV-1 PR by Zn^{+2} was observed to be competitive or noncompetitive depending on the substrate; however, in neither case did loss of activity involve disruption of the dimeric structure of the protease.[12] Our simulation of Zn^{+2}-bound HIV-1 PR shows no weakening of the dimer. In fact, the zinc-bound form of the enzyme is more similar to the crystallographic structure than the unbound protease having fully charged aspartate residues. It is possible that interresidue repulsions between the aspartates in their fully ionized form destabilizes the dimeric structure in solution to some degree. This view is consistent with experimental studies by Cheng et al.[35] that illustrate the dissociative nature of the HIV-1 protease at pH 7 and above. In crystallographic structures of the HIV-1 protease,[6,7] and the related protease from the Rous sarcoma virus,[36,37] there is electron density for perhaps a water molecule near the catalytic aspartate residues. It is probable that interaction of a water molecule or possibly an ion could stabilize the dimer by binding the carboxylates at the interface. Experimental evidence has indicated that the dimeric structure is stabilized in high salt concentration,[35] a not unexpected result because hydrophobic interactions also play an important role at the dimer interface. The overall simulation results, indicate that Zn^{+2} can bind stably with the catalytic aspartate residues of the HIV-1 protease without significantly disrupting the overall structure. These results are consistent with experimental studies, and taken together suggest that the site of Zn^{+2} binding that leads to catalytic inhibition is in the active site.

Conclusion

Simulations of the HIV-1 protease in solution have been performed both in the presence and absence of bound zinc. Preliminary potential energy considerations based on the crystallographic structure suggest a favorable binding site for a Zn^{+2} ion is located in the active site at the catalytic aspartate residues. Experimental studies also suggest that the Zn^{+2} binding site responsible for inactivation of the protease occurs in this region.[12] Molecular dynamics simulations indicate the ion remains stably bound, coordinating the carboxylate side chains of the catalytic aspartate residues. Interaction of the zinc in this position did not disrupt the dimeric structure of the protein or significantly alter the structure of the active site. These data are consistent with experimental observations of Zn^{+2}-bound HIV-1 protease[12] and give further evidence that this is the binding site that leads to inhibition. A refined model of the active site based on quantum mechanical calculations indicates zinc coordination is monodentate with each catalytic aspartate, with at least two ligand positions available to water or other nonprotein substituents. Development of chemically modified zinc compounds that exploit the potentially free ligand positions may provide a possible strategy for the design of new inhibitors or drugs against HIV-1 PR.

Acknowledgments

The authors thank Dr. A. Wlodawer for providing several crystallographic structures and acknowledge grants of supercomputer time from the National Cancer Institute and the North Carolina Supercomputing Center (a division of MCNC). D.M.Y. thanks the University of North Carolina Medical School for support through the MD/PhD program. L.G.P. thanks NIEHS, RTP, NC, for support for this project and acknowledges NIH Grant HL27995. The authors also thank Howard Smith at NIEHS for essential computer graphics assistance and Drs. Nobuko Hamaguchi and Paul Charifson for advice on the manuscript.

References

1. T. D. Meek, B. D. Dayton, B. W. Metcalf, G. B. Dreyer, J. E. Strickler, J. G. Gorniak, M. Rosenberg, M. Moore, V. W. Magaard, and C. Debouck, *Proc. Natl. Acad. Sci. USA*, **86,** 1841 (1989).
2. C. Debouck, J. G. Gorniak, J. E. Strickler, T. D. Meek, B. W. Metcalf, and M. Rosenberg, *Proc. Natl. Acad. Sci. USA*, **84,** 8903 (1987).
3. J. Huff, *J. Med. Chem.*, **34,** 2305 (1991).
4. C. Debouck, *AIDS Res. Human Retrovir.*, **8,** 153 (1992).
5. M. A. Navia, P. M. D. Fitzgerald, B. M. McKeever, C. T. Leu, J. C. Heimbach, W. K. Herber, I. S. Sigal, P. L. Darke, and J. P. Springer, *Nature*, **37,** 615 (1989).
6. A. Wlodawer, M. Miller, M. Jaskólski, B. K. Sathyanarayana, E. Baldwin, I. T. Weber, L. M. Selk, L. Clawson, J. Schneider, and S. B. H. Kent, *Science*, **245,** 616 (1989).
7. R. Lapatto, T. Blundell, A. Hemmings, J. Overington, A. Wilderspin, S. Wood, J. R. Merson, P. J. Whittle, D. E. Danley, K. F. Geoghegan, S. J. Hawrylik, S. E. Lee, K. G. Scheld, and P. M. Hobart, *Nature*, **342,** 299 (1989).
8. A. Wlodawer and J. W. Erickson, *Annu. Rev. Biochem.*, **62,** 543 (1993).

9. L. J. Hyland, T. A. Tomaszek, and T. D. Meek, *Biochemistry*, **30,** 8454 (1991).
10. E. Ido, H. Han, F. J. Kezdy, and J. Tang, *J. Biol. Chem.*, **266,** 24359 (1991).
11. T. Inagami, In *Biochemical Regulation of Blood Pressure*, John Wiley & Sons, New York, 1981, p. 39.
12. Z. Zhang, I. Reardon, J. Hui, K. O'Connell, R. Poorman, A. Tomasselli, and R. Heinrikson, *Biochemistry*, **36,** 8717 (1991).
13. S. J. Weiner, P. A. Kollman, D. A. Case, U. C. Singh, C. Chio, G. Alagona, S. Profeta, and P. Weiner, *J. Am. Chem. Soc.*, **106,** 765 (1984).
14. C. K. Foley, L. G. Pedersen, P. S. Charifson, T. A. Darden, A. Wittinghofer, E. F. Pai, and M. W. Anderson, *Biochemistry*, **31,** 4951 (1992).
15. S. J. Weiner and P. A. Kollman, *J. Comp. Chem.*, **7,** 230 (1986).
16. W. L. Jorgensen, J. Chandrasekhar, J. D. Madura, R. W. Impey, and M. L. Klein, *J. Chem. Phys.*, **79,** 926 (1983).
17. T. Lybrand, J. McCammon, and G. Wipff, *Proc. Natl. Acad. Sci. USA*, **83,** 833 (1986).
18. L. Bartolotti, L. Pedersen, and P. Charifson, *J. Comp. Chem.*, **12,** 1125 (1991).
19. W. E. Harte, Jr., S. Swaminathan, M. M. Mansuri, J. C. Martin, I. E. Rosenberg, and D. L. Beveridge, *Proc. Natl. Acad. Sci. USA*, **87,** 8864 (1990).
20. D. York, T. Darden, L. Pedersen, and M. Anderson, *Biochemistry*, **32,** 1443 (1993).
21. J. Stewart, *J. Comp.-Aided Mol. Design*, **4,** 1 (1990).
22. J. Stewart, *J. Comp. Chem.*, **12,** 320 (1991).
23. M. W. Jurema and G. C. Sheilds, *J. Comp. Chem.*, **14,** 89 (1993).
24. M. Karplus and G. Petsko, *Nature*, **347,** 631 (1990).
25. W. E. Harte Jr., S. Swaminathan, and D. L. Beveridge, *Proteins*, **13,** 175 (1992).
26. W. Kabsch and C. Sander, *Biopolymers*, **22,** 2577 (1983).
27. I. T. Weber, *J. Biol. Chem.*, **265,** 10492 (1990).
28. J. Burgess, *Ions in Solution*, John Wiley & Sons, New York, 1988.
29. C. J. Carrell, H. L. Carrell, J. Erlebacher, and J. P. Glusker, *J. Am. Chem. Soc.*, **110,** 8651 (1988).
30. J. Tözér, I. T. Weber, A. Gustchina, I. Bláha, T. D. Copeland, J. M. Louis, and S. Oroszlan, *Biochemistry*, **31,** 4793 (1992).
31. J. Koryta, *Medical and Biological Applications of Electrochemical Devices*, John Wiley & Sons, New York, 1980.
32. T. Woon, R. Brinkworth, and D. Farlie, *Int. J. Biochem.*, **24,** 911 (1992).
33. L. S. Beese and T. A. Steitz, *EMBO J.*, **10,** 25 (1991).
34. M. M. Yamashita, L. Wesson, G. Eisenman, and D. Eisenberg, *Proc. Natl. Acad. Sci. USA*, **87,** 5648 (1990).
35. Y. Cheng, F. Yin, S. Foundling, D. Blomstrom, and C. Kettner, *Biochemistry*, **87,** 9660 (1990).
36. M. Miller, M. Jaskólski, J. K. Rao, J. Leis, and A. Wlodawer, *Nature*, **337,** 576 (1989).
37. M. Jaskólski, M. Miller, J. K. Mohana Rao, J. Leis, and A. Wlodawer, *Biochemistry*, **29,** 5889 (1990).